Square-Wave Adsorptive Cathodic Stripping Voltammetric Determination of Trace Palladium Using 4-(2-Thiazolylazo)-Resorcinol

Abdelgany Hamza[a], Amal A. Bahaffi[a], Abdulaziz A. Al-Sibaai[a], and Mohammad S. El-Shahawi[a, *, **]

[a]*Chemistry Department, Faculty of Science, King Abdulaziz University, P.O. Box 80203, Jeddah, 21589 Saudi Arabia*
*e-mail: malsaeed@kau.edu.sa
**e-mail: mohammad_el_shahawi@yahoo.co.uk

Abstract—A square-wave adsorptive cathodic striping voltammetry method has been established for trace determination of palladium. The method was based on the adsorptive enrichment of palladium(II)−4-(2-thiazolylazo)-resorcinol (**TAR**) complex at the hanging mercury drop electrode at pH 7−8 versus Ag/AgCl electrode. At the optimized stripping parameters of pH, scan rate, potential accumulation, deposition time, pulse amplitude, frequency, pulse width and TAR concentration, the established method exhibited good sensitivity and remarkable linear range of 0.5−53 µg/L for Pd. The limits of detection and quantification were 0.15 and 0.5 µg/L, respectively, with relative standard deviation of ±2.1% ($n = 3$) at 10 µg/L Pd. The developed method was judged by quantification of Pd in certified reference material (IAEA-Soil-7) and using inductively coupled plasma-mass spectrometry. The calculated Student t and F values did not exceed the tabulated t (2.18) and F (3.63) at $P = 0.05$, revealing no significant difference between the two methods. The method was free from the interference from most of the common anions, cations and surfactants present in water. The method was satisfactorily applied to the quantification of Pd in road dust and water samples.

Keywords: palladium determination, square wave cathodic stripping voltammetry, hanging mercury drop electrode, electrode kinetics and mechanism, water and roadside dust samples

DOI: 10.1134/S1061934821030059

Recent years have seen wide use and various applications of platinum group metals (**PGMs**), e.g., Pd, Pt, and Rh, in the jewelry industry, autocatalytic converters in motor vehicles and in some industrial processes. These applications have increased PGM contents in our environment [1]. PGMs are present at low crustal abundance (≈1 ng/g). Pd most likely occurs in the Earth's crust and is associated with one or more of the other PGMs in addition to other elements [2]. Palladium has been used in brazing alloys, petroleum, electrical industries, catalytic chemical reactions and converters in palladium-based motor vehicles [3].

In fresh water, salt water, soil, sewage sludge, ambient air in urban areas, Pd catalysts are used, where Pd content generally ranges from 0.4 to 22 ng/L, 19−70 pg/L, <0.7−47 µg/kg, 18−260 µg/kg and below 110 pg/m^3 [4], respectively. Pd concentration is in the range of 0.006−<0.3 µg/L in urine of adults and the human average dietary intake of Pd appears to be up to 2 µg/day [5], whereas in drinking water Pd concentration is usually <24 ng/L. The maximum allowable levels of Pd by World Health Organization (**WHO**) in surface and drinking water were set at 0.01 and 0.005−30 mg/L [3], respectively. Thus, the enlargement of

low cost and simple procedures for the determination of PGMs (Ru, Ir, Pt, Rh, Os) at trace levels is emergent because of their use in medicine, micromechanics and chemical engineering. Monitoring Pd at trace levels in surface waters, soil surfaces and plant samples has been rapidly increasing [5].

Trace levels of Pd together with the high contents of interfering matrix components often require a separation and/or pre-concentration step combined with a matrix separation [6]. Numerous methods such as inductively coupled plasma-optical emission spectroscopy, inductively coupled plasma−mass spectrometry (**ICP−MS**), electrospray ionization mass spectrometry, electrothermal atomic absorption spectroscopy, solution scanometric technique and fluorescence have been conveyed for Pd determination [6−22]. Most of these methods suffered from several disadvantages, e.g., low enrichment step, high cost of the instruments, complexity, and the need of degree of proficiency for their proper operation. Thus, the development of highly sensitive, reliable, low cost and easy-to-function methods for routine Pd determination is of prime importance in recent years.

Recently, stripping voltammetric methods have been reported for sensitive Pd determination [2, 22—33]. Square-wave voltammetry represents one of the most popular and most exploited techniques in the family of the pulse voltammetric techniques because of its excellent sensitivity and selectivity, low detection limits, good accuracy and precision and inexpensive and portable instrumentation [32, 34]. Flexible screen-printed unmodified carbon electrode has been reported recently for Pd determination by Velmurugan et al. [33]. To this point, 4-(2-thiazolylazo)-resorcinol (**TAR**) reagent has not been used for voltammetric determination of Pd^{2+} and other PGMs at the hanging mercury drop electrode (**HMDE**). Despite some associated noxiousness, HMDE is considered to be extremely reliable, stable and reproducible for the quantification of organic pollutants and trace and ultra-trace metal speciation in marine water [23, 24, 34]. HMDE provides basic understanding of the electrochemical reduction process with wide potential window in the cathodic region. HMDE is also non-toxic as long as packing and discarding of Hg are undertaken in a safe manner [34—37]. Regardless of the expansion of surface modified electrodes, the use of Hg electrodes will stay in future for studying new classes of pesticides and potential targets in many biochemical and biological systems and complicated environmental matrices. Thus, this study is focused on developing a low cost and precise square wave adsorptive cathodic striping voltammetry (**SW CSV**) procedure for Pd determination at trace level using 4-(2-thiazolylazo)-resorcinol at the HMDE, revising possible interference from other metal ions and common surfactants, testing the analytical utility of the proposed procedure for Pd determination in water samples and finally assigning the nature and mechanism of the electrode reaction.

EXPERIMENTAL

Reagents and materials. Analytical reagent and supra grade chemicals were used without further purification. All glassware's and electrochemical cell used in this study were pre-cleaned with HNO_3 (20%, w/v), soaked in acetone for at least 15 min, then washed with deionized water and dried at 120°C. Nalgene low-density polyethylene bottles were used for storage of the stock solutions and real water samples. TAR, sodium dodecyl sulfate, tetraheptylammonium chloride and Triton X-100 reagents were purchased from Sigma-Aldrich (Dublin, Ireland). $Pd(NO_3)_2$ was purchased from BDH (Poole, England). A stock solution (1.0 mg/mL) of Pd was prepared from $Pd(NO_3)_2$ in ultra-pure water. A series of more diluted solutions of Pd^{2+} ions was prepared in deionized water. 1.0 mM TAR stock solution in methanol was prepared and stored in refrigerator. Double-distilled water was used for preparation of diluted solutions. Working solutions of sodium dodecyl sulfate, tetraheptylammonium

chloride and Triton X-100 (10%, w/v) were prepared in water The competent cations (as their nitrate and/or chloride salts), anions (as Na or K salts) and surfactants were purchased from Fluka A.G. (Buchs SG, Switzerland). Britton—Robinson (**B—R**) buffer (pH 2—11) was used as a supporting electrolyte. Concentrated HF, HCl and HNO_3 acids were purchased from Merck (Darmstadt, Germany). A certified reference material (**CRM**, IAEA-Soil-7) was purchased for method validation.

Apparatus. Voltammetric (cyclic, linear and differential pulse cathodic stripping) measurements were performed on a Metrohm 757 VA trace analyzer and a 747 VA stand (Basel, Switzerland). A Perkin Elmer inductively coupled plasma mass spectrometer (Sciex model Elan DRC II, USA) was used for measuring trace and ultra-trace concentrations of Pd under the optimized parameters and for validation of the developed SW CSV method for Pd determination. A Perkin Elmer (Lambda EZ-210) double beam spectrophotometer (190—1100 nm) with 1 cm (path width) quartz cell was used for recording the electronic spectra of the reagent TAR and its Pd(II) complex. A Perkin Elmer Fourier-transform infrared spectrometer (**FTIR**) spectrometer 100 series (Beaconsfield, Bucks, UK) was used for recording the IR spectra of TAR and its Pd(II) complex. A CEM microwave system (Mars model, 907500, USA) was used for the digestion of the CRM (IAEA-Soil-7). A three-compartment voltammetric cell (10 mL) incorporating the HMDE with a drop surface area of 5 mm^2 as a working electrode, double-junction Ag/AgCl (3 M KCl) as a reference electrode and Pt wire (BAS model MW-1032) as a counter electrode, respectively, was used. A mechanical mini-stirrer and a capillary to supply N_2 as an inert gas were used. A digital-micro-pipette (10—100 μL, Volac) was used for transferring the sample solutions to the electrochemical cell. The peak currents were measured using the tangent-fit method at room temperature. An Orion pH-meter and a Milli-Q Plus water purification system (Milford, MA, USA) were used.

Recommended square wave adsorptive cathodic striping voltammetry procedure. An accurate volume (10 mL) of B—R buffer (pH 7) was transferred into the cell, where the electrodes were immersed in the test solution and pure N_2 gas was passed for 15 min before recording voltammograms. The scans were initiated from applied potential of 0.0 to −1.5 V versus Ag/AgCl electrode. After recording the voltammogram of the supporting electrolyte, an accurate volume (150 μL) of 0.1 mM TAR was transferred into the cell (10 mL) to provide a final concentration of 1.5 μM. A stream of pure N_2 was then passed through the solution for 5.0 min before recording voltammogram. The stirrer was then stopped and after 10 s of quiescence, the voltammogram was recorded at 180 s accumulation time, 0.15 V deposition potential, 0.0 V starting potential,

50 mV pulse amplitude and 60 mV/s scan rate. The background SW CSV of the supporting electrolyte and the blank (TAR) solutions were recorded. An accurate volume (20 μL) of Pd^{2+} solution (1.2×10^{-7} M) was added to the cell and the solution was purged with N_2 gas for 2–3 min. The SW CSV was repeated with a new Hg drop under the same experimental conditions in the presence of various known concentrations of Pd (20–100 μL). The stirrer was stopped and after 10 s of quiescence, scan was initiated from 0.0 to −1.5 V. The peak current of Pd was measured at −0.43 V and Pd concentration was determined from the difference between the cathodic peak current before and after addition of Pd^{2+} ions to TAR solution. Following these procedures, the influence of the competent cations was studied, and cyclic voltammetry (**CV**) at various scan rates (0.02–1 V/s) versus Ag/AgCl electrode was tested. A stream of nitrogen was passed through the solution for 5 min before each experiment to remove oxygen.

Analytical applications. *Analysis of certified reference material and road dust.* An accurate weight (0.13–0.15 g (±0.01 g)) of the CRM sample (IAEA-Soil-7) was digested and re-dissolved in dilute HNO_3 (5.0 mL, 1.0 M) as reported [38]. The test solution was then filtered through a Whatman filter paper (Grade 41), diluted with deionized water and subsequently transferred quantitatively into a volumetric flask (25.0 mL). An accurate volume (5 mL) of the digested sample adjusted to pH 7 with few drops of NaOH (1.0 M) and B–R buffer (pH 7) were transferred to the electrochemical cell. SW CSVs were then recorded after each addition of various known concentrations of Pd at the optimized parameters by applying a negative potential from 0.0 to −1.5 V versus Ag/AgCl. At ~0.43 V, the peak current was measured and the change in its value was used for constructing the linear plot of standard addition of Pd. The content of representative ion in the CRM sample was estimated from the linear plot of the standard addition.

Determination of palladium in road dust samples. Samples collected from the surface of the roadside dust of the busy streets of Jeddah City of heavy and light traffic were initially dried at 110°C for 2 h, grounded through a 200-mesh sieve and homogenized. Accurate weights of the samples were individually digested in Teflon beakers in the presence of various known Pd^{2+} concentrations as reported for the CRM [38]. The solid residues were re-dissolved in water, centrifuged, filtered through a 0.45 μm membrane filter, transferred to the measuring flask (25.0 mL) and completed to the mark with HNO_3 (0.5 M) and finally analyzed as described for the CRM sample.

Determination of palladium in environmental water samples. Tap water sample was collected from the laboratory of Department of Chemistry located in King Abdulaziz University campus (Jeddah). Wastewater samples were obtained from various collection points in Jeddah, Saudi Arabia. A known concentration of Pd^{2+} (0–30 μg/L) was spiked into the water sample, filtered through a 0.45 μm cellulose acetate membrane filter and subjected to UV mineralization for 6 h. Known volume (10.0 mL) of the water sample was transferred to the cell and adjusted to pH 7. The test sample was analyzed following the recommended procedures described above after adding few drops of ethylenediaminetetraacetic acid (**EDTA**) (2%, w/v). The current height displayed by the test solution before and after addition of various volumes of standard palladium(II) was then measured and used for determining palladium(II) via the linear plot of the standard addition. For method validation, these samples were also analyzed by ICP–MS under the optimized operational parameters.

RESULTS AND DISCUSSION

Electronic spectra of 4-(2-thiazolylazo)-resorcinol and its Pd^{2+} complex. The spectrum of the Pd-TAR complex showed one well-defined absorption peak at λ_{max} of 443 and 459 nm, respectively. The observed color change and the progressive bathochromic shift in the electronic spectra of Pd−TAR complex suggest formation of Pd−TAR complex. The stoichiometry and stability constant of the formed Pd−TAR chelate as calculated from the continuous variation at 459 nm [39] were found equal to 1 : 2 (Pd^{2+} : TAR) molar ratios and 5×10^{11} at 25°C, respectively. FTIR spectra (4000–400 cm^{-1}) for TAR and its Pd^{2+} complex were recorded. The band at 1587 cm^{-1} assigned to ν (N=N) of azo group of TAR was shifted to lower frequency (56 cm^{-1}) on complex formation indicating coordination of azo group (N=N) nitrogen on complex formation with Pd [40, 41]. The appearance of the band at 452–531 cm^{-1} in the complex corresponding to the ν (Pd−N) also supported the coordination of azo group of TAR [40, 41]. The observed blue shift (63 cm^{-1}) of the ν (C−O) stretching band in the complex [41] confirmed the participation of the deprotonated phenolic OH group. The appearance of the band at 527–530 cm^{-1} due to ν (Pd−O) stretching vibration added further support to the participation of phenolic OH. Thus, TAR coordinates to Pd^{2+} in a bidentate fashion via azo and phenolic OH group. Hence, the most probable structure of Pd^{2+}−TAR complex is PdL_2 (where L corresponds to TAR−H).
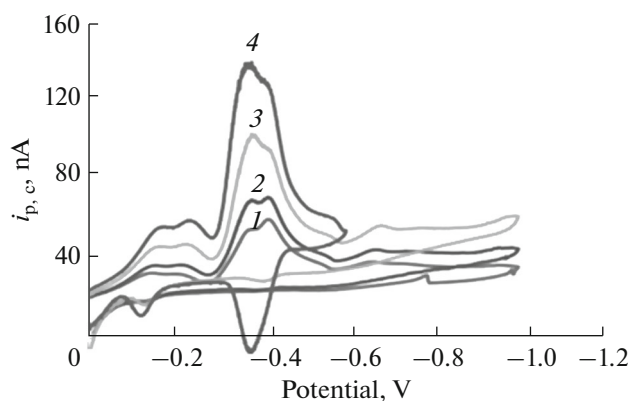
Redox behavior of palladium(II)-4-(2-thiazolylazo)-resorcinol complex. Based on the stability constant of Pd−TAR complex, a comprehensive SW CSV study of TAR in the absence and presence of Pd^{2+} ions using B−R buffer in a wide pH range of 2−10 was studied. The voltammograms of the supporting electrolyte and TAR, i.e., the background, revealed no cathodic peaks in the studied potential range from
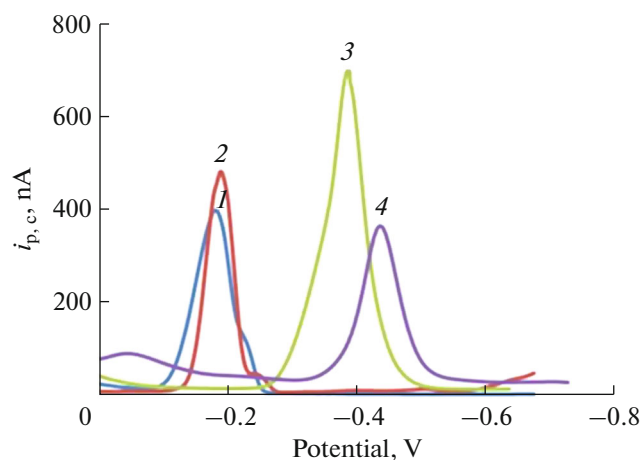
Fig. 1. SW CSV of Pd^{2+}–TAR complex in B–R buffer at various pH at the HMDE versus Ag/AgCl: TAR concentration of 9×10^{-8} M, Pd^{2+} concentration of 1.6×10^{-6} M, scan rate of 0.1 V/s, pulse amplitude of 60 mV. pH: (*1*) 4, (*2*) 5, (*3*) 7, (*4*) 8.

Fig. 2. CVs of Pd^{2+}–TAR at various scan rates (30–100 mV/s) at pH 7 at HMDE versus Ag/AgCl: TAR concentration of 1.6×10^{-6} M and Pd^{2+} concentration of 1×10^{-7} M. Scan rate, mV/s: (*1*) 30, (*2*) 45, (*3*) 60, (*4*) 100.

0.0 to −1.0 V versus Ag/AgCl electrode. The instability of the electrogenerated species and/or the presence of hydrogen at the surface of the HMDE may account for the observed trend [31, 32]. On the other hand, on adding Pd^{2+} ions to TAR solutions at pH 4.0–8.0, one well-defined cathodic peak was observed in the range from 0.0 to 0.6 V versus Ag/AgCl electrode. Representative SW CSVs at pH 4–8 are shown in Fig. 1. The observed cathodic peak was safely assigned to the reduction of azo group (−N=N−) of TAR center in Pd–TAR complex where $2H^+/2e$ are exchanged in one-step producing the corresponding hydrazo compound [24, 42]. On increasing the solution pH, the $E_{p,c}$ at −0.23 V shifted to more negative values showing the irreversible nature of the reduction process and the electrode reaction involving hydrogen ions [24, 43, 44].

The dependence of the cathodic peak potential ($E_{p,c}$) on pH can be explained by a direct exchange step of $4H^+/4e$ [37, 45] with splitting of −N=N− group producing the corresponding hydrazo compound −NH−NH₂ [42]. At pH >8, the observed cathodic peak was less intense and disappeared due to the instability and/or hydrolysis of the electrogenerated Pd–TAR species and the unfavorable adsorbability of the generated species at the HMDE [44, 45]. The cathodic peak current ($i_{p,c}$) increased on raising the solution pH and reached maximum at pH 7. Thus, a buffer solution of pH 7 was carefully chosen in the subsequent work. Moreover, at this pH, constant, reproducible, sharp and high cathodic peak current at −0.43 V was noticed. The plot of the change of the $E_{p,c}$ versus pH was linear following the regression equation: $E_{p,c} = -0.124\text{pH} + 0.661$ ($R^2 = 0.9787$).

The CVs of Pd(II)−TAR complex at the HMDE at pH 7 at various scan rates (0.02−1.0 V/s) (log ν) versus Ag/AgCl electrode were recorded. Representative CVs are shown in Fig. 2. At scan rates ≤0.1 V/s, the CV showed two ill-defined cathodic peaks in the potential range from −0.10 to −0.37 V and another ill-defined cathodic peak in the range from −0.65 to −0.75 V. A well-defined cathodic peak at −0.45 V was also observed. On reversing the scan, two anodic peaks at −0.37 and −0.10 V were observed (Fig. 2).

The irreversible nature of the cathodic peak at −0.45 V was suggested from the linear plot of the cathodic peak potential ($E_{p,c}$) versus log ν at pH 7 [46, 47]. The peak–peak potential separation (ΔE_p) between the anodic peak at −0.32 V and the small cathodic peak at −0.45 V increased on raising the scan rate confirming the irreversible nature of the electrode reaction, and the product of the reduction step undergoes a very slow follow-up chemical reaction and the protonation reaction is very fast and/or complete in solution medium [45, 46]. Thus, the potential ($E_{p,a}$) of the electrode process can be defined by the Laviron Eq. (1) [47]:

$$E_p = E^{\circ\prime} + \frac{2.303RT}{\alpha nF} \log \frac{RTK^\circ}{\alpha nF} + \frac{2.303RT}{\alpha nF} \log \nu, \quad (1)$$

where K° is the standard heterogeneous rate constant of the electrode reaction, α is the transfer coefficient, n is the number of electrons transferred, ν is the scan rate and $E^{\circ\prime}$ is the formal redox potential. Other symbols have their usual meanings. Taking $R = 8.314$ J/(K mol), $T = 298$ K and $F = 96\,485$ C, the value of αn was easily calculated from the slope of the linear plot of $E_{p,c}$ versus logν. Assuming the number of the electrons involved in the reduction step (n_α) equal to 2, the computed value of α was found equal to 0.52 ± 0.01 confirming the irreversible nature of the reduction process at the HMDE surface. This value is not near the theoretical value (1.0) expected when there is an adsorption

process at the HMDE [44–46]. The irreversible nature was also confirmed from the linear plot of log $i_{p,c}$ versus logν at pH 7 at the HMDE [45, 46]. The plot of the cathodic peak current ($i_{p,c}$) versus square root of the scan rate ($\nu^{1/2}$) was also linear showing that the reduction step was diffusion-controlled [45–47].

The variation of the current function with the scan rate of Pd(II)–TAR complex at −0.45 V is an important diagnostic criterion for assigning the mechanism of the electron transfer [46, 47]. The current function increased on increasing the ν, indicating that the ECE (chemical reaction coupled between two charge-transfer processes) type mechanism electrode process was favorable and EE mechanism was excluded [43, 45]. The product of the reduction process also undergoes a very rapid follow-up chemical reaction [45, 46]. The surface coverage (Γ) of the electroactive complex species of Pd–TAR at the HMDE was computed from the linear plot of $i_{p,c}$ at 0.43 V versus square root of ν using the Eq. (2) [43, 46]:

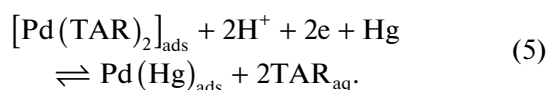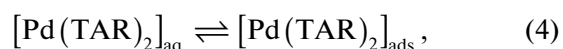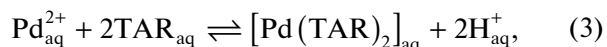$$i_{p,c} = \frac{n^2 F^2 A \Gamma \nu}{4RT}, \quad (2)$$

where n is the number of electrons involved in the electrode reaction, A is the geometric surface area of HMDE and Γ (mol/cm^2) is the surface coverage [46, 47]. Assuming n equal to 2, the calculated value of Γ was found as $3.8 \times 10^{-10} \pm 0.05$ mol/cm^2 recommending the possible use of SW CSV for trace determination of Pd.

Optimization of the analytical parameters. The SW CSV behavior of Pd–TAR chelate at various pHs and the sensitivity of the established cathodic peak and $i_{p,c}$ at −0.43 V at the HMDE revealed the utility of this reagent for developing a convenient method for Pd^{2+} determination. At pH 7, one well defined and reproducible cathodic peak at −0.43 V was observed (Fig. 2). At pH > 5, TAR easily dissociated and participated in complex formation with Pd(II). Hence, as mentioned above, the supporting electrolyte solution was adjusted to pH 7 in the next experiments.

A detailed study on the influence of the deposition potential (−0.1–0.2 V) at pH 7 on the $i_{p,c}$ at −0.43 V was studied. The results are illustrated in Fig. 3a. The $i_{p,c}$ at −0.43 V increased as the potential of the electrode became less negative (0.13–0.15 V) and a clear drop in the peak current was noticed at positive potentials (>0.15 V). At pH 7, Pd–TAR complex could bear negative charge and its adsorption was most likely favored at potential less than 0.15 V. Thus, a deposition potential of 0.15 V was established in the next work. At this potential, the cathodic peak current was much more developed, resolved, symmetric and sharp. Thus, in the following work, the deposition was adopted at 0.15 V. The overall signal can safely be assigned as follows (Eqs. (3)−(5)):
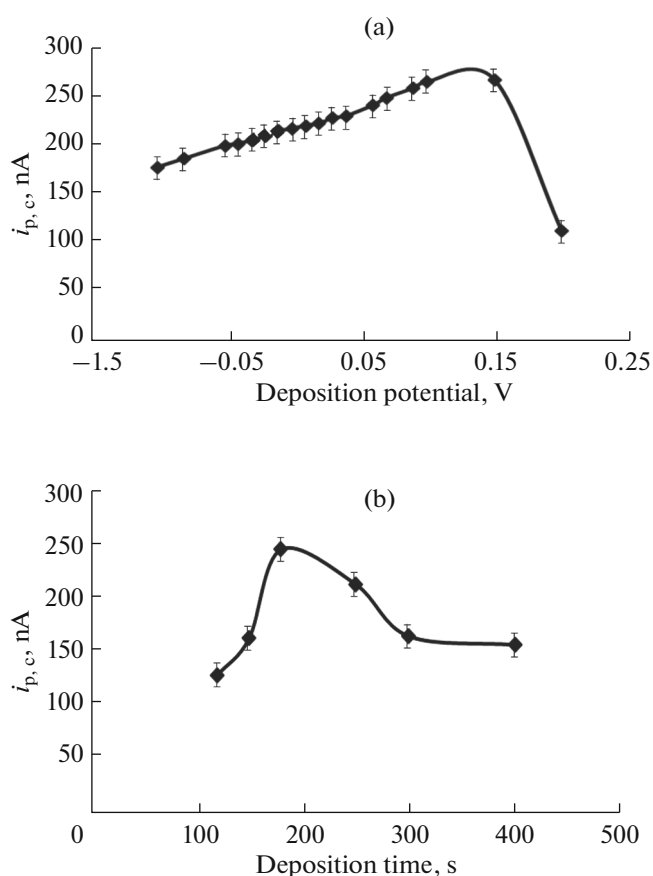

Fig. 3. Plots the cathodic peak current of Pd^{2+}–TAR complex at the HMDE versus deposition potential (a) and deposition time (b): TAR concentration of 9×10^{-8} M, Pd(II) concentration of 1.6×10^{-6} M, accumulation time of 180 s, pulse amplitude of 0.05 V and scan rate of 0.05 V/s.

$$Pd_{aq}^{2+} + 2TAR_{aq} \rightleftharpoons \left[Pd\left(TAR\right)_2\right]_{aq} + 2H_{aq}^+, \quad (3)$$

$$\left[Pd\left(TAR\right)_2\right]_{aq} \rightleftharpoons \left[Pd\left(TAR\right)_2\right]_{ads}, \quad (4)$$

$$\left[Pd\left(TAR\right)_2\right]_{ads} + 2H^+ + 2e + Hg$$
$$\rightleftharpoons Pd\left(Hg\right)_{ads} + 2TAR_{aq}. \quad (5)$$

Deposition time represents the most important criteria in stripping voltammetric procedures that has a pronounced effect on sensitivity and/or linear dynamic range. Hence, the influence of deposition time (100−400 s) on the cathodic peak current at −0.43 V was studied. The $i_{p,c}$ increased with increasing deposition time up to 180 s, decreased at longer deposition time (>200 s) and remained constant at longer time (Fig. 3b). This behavior could be attributed to saturation of the adsorbed film of the complex on the electrode surface. Thus, it can be concluded that the chemical equilibrium between the electrode and the complex species of Pd(II) at the employed pH 7 was achieved at a deposition time <200 s. Thus, deposition time of 200 s was adopted.
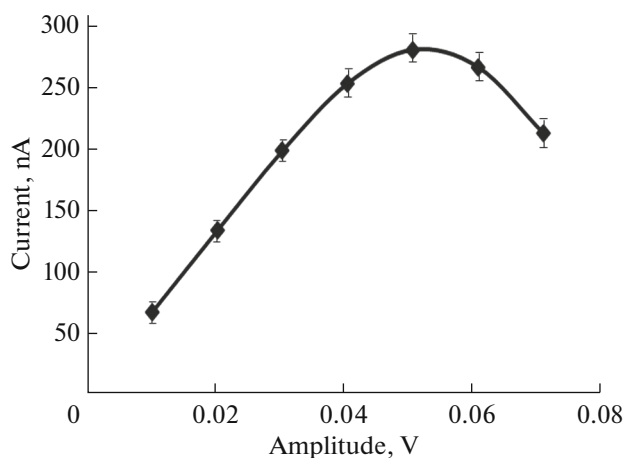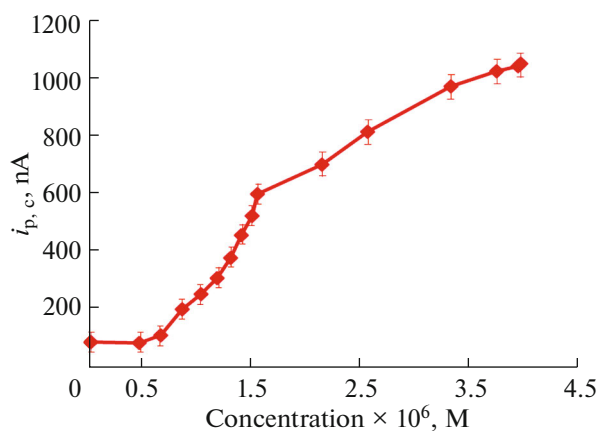
Fig. 4. Plot of cathodic peak current at pH 7 at HMDE versus pulse amplitude: deposition potential of 0.15 V versus Ag/AgCl electrode, deposition time of 200 s, scan rate of 0.05 V/s.

Fig. 5. Plot of cathodic peak potential at pH 7−8 at HMDE versus of TAR concentrations. Deposition potential of 0.15 V versus Ag/AgCl reference electrode, deposition time of 200 s, scan rate of 0.05 V/s and pulse amplitude of 50 mV.

The effect of scan rate (0.03−0.1 V/s) on the $i_{p,c}$ was studied at a peak potential of −0.47 V. The $i_{p,c}$ gradually increased on raising the scan rate up to 0.1 V/s. However, good signal to background current, sharp and peak symmetry were achieved at 0.05 V/s. Thus, the sweep rate was adjusted at 0.05 V/s in the next experiments.

The influence of pulse amplitude is crucial since it has a combined effect on the SW CSV response of Pd−TAR species at the optimized pH. Thus, the effect of pulse amplitude (0.01−0.07 V) on the $i_{p,c}$ under the optimized conditions was studied. The results are demonstrated in Fig. 4. An increase in the $i_{p,c}$ was noticed on increasing the pulse amplitude up to 0.05 V and decreased at higher values. At a pulse amplitude of 0.05 V, best sensitivity and instrumental setting of the $i_{p,c}$ to background current characteristics were achieved, whereas at a pulse height >0.05−0.09 V, broadening of the SW CSVs cathodic peak was noticed with a shift to more negative values. On the other hand, the peak width further increased on increasing pulse amplitude which sloped the background current signal and made SW CSV measurements difficult. Thus, a pulse amplitude of 0.05 V was selected in the next work.

The effect of frequency on the SW CSV mode is of prime importance, thus the effect of frequency (10−40 Hz) was studied. A well resolved and maximum stripping peak current was noticed in the frequency range of 30−40 Hz. Thus, a frequency of 40 Hz was chosen for the consequent experiments.

The effect of TAR concentration (1.0×10^{-8}−3×10^{-6} M) on the $i_{p,c}$ at $E_{p,c}$ −0.43 V and pH 7 was critically studied at known palladium concentration (5×10^{-7} M). The $i_{p,c}$ increased linearly and a well distinct break point was noticed at TAR concentration slightly

higher than 1.0×10^{-6} M (Fig. 5). It is worth noting that this concentration (1.0×10^{-6} M) of TAR was approximately twice the concentration of Pd^{2+}. Thus, the structure of the adsorbed complex species most likely has the chemical formula of $Pd(TAR)_2$. At TAR concentration higher than 1.0×10^{-6} M, the value of $i_{p,c}$ increased but less pronounced than with lower TAR concentration. The specific competitive adsorption of $Pd(TAR)_2$ with the free TAR on the surface of the HMDE may account for the observed trend. Moreover, non-adsorptive of Pd^{2+} species at lower TAR concentration may also participate in the observed trend. Thus, TAR concentration of 1.5×10^{-6} M was implemented in the succeeding measurements as a compromise between good sensitivity and complex stability.

Analytical performance criteria. Under the optimal parameters of pH 7, deposition potential (0.15 V), accumulation time (200 s), scan rate (0.05 V/s), pulse-amplitude (−0.06 V) and TAR concentrations (1.5×10^{-6} M), the plot of $i_{p,c}$ at −0.43 V versus Pd^{2+} concentrations was linear in the range of 0.5−53 μg/L with a regression coefficient (R^2) of 0.999. At higher Pd^{2+} concentration, the cathodic peak current leveled off because of adsorption saturation at the HMDE [43–47]. The values of limits of detection (**LOD**) and quantification (**LOQ**) were established using the Eqs. (6), (7):

$$LOD = \text{Blank mean} + 3SD, \qquad (6)$$

$$LOQ = 3.33 \times LOD. \qquad (7)$$

where SD is the standard deviation of the blank, as reported by Konieczka and Namieśnik [48], and the values of 0.15 and 0.5 μg/L, respectively, were obtained. Precision, in terms of repeatability, was typically below 4% for cathodic peak current and 0.1% for

Table 1. Comparison of the developed SW CSV method analytical performance with some reported spectrometric and electrochemical assays for palladium determination

Method[a]	LOD, µg/L	LDR, µg/L	Remark	Reference
DLLME–GFAAS	1.0	0.025–0.500	Non-selective, time consuming reagent, easy colorimetric read-out	[13]
DLLME–FAAS	0.02	–	Requires sample preparation, use of chlorinated organic solvent, time consuming	[14]
MASPE–ICP–MS	0.53	0.050–2.500	Too expensive, high LOD, complex, time consuming	[15]
DP CSV	0.04	–	Sensitive, multiple step methodology	[24]
DP CSV	0.05	0.2–32.5	Expensive hybrid raw materials, needs high technical skills	[2]
FAAS	0.15	1–80	Preconcentration on SPE, time consuming and costly	[49]
SW CSV	0.15	0.5–53	Rapid and easy read-out	This work

Abbreviations: LDR—linear dynamic range, DLLME–GFAAS—dispersive liquid–liquid microextraction–graphite furnace atomic absorption spectrometry, MASPE–ICP–MS—microwave-assisted solid phase extraction procedure coupled to inductively coupled plasma mass spectrometry, SPE—solid phase extraction, FAAS—flame atomic absorption spectrometry.

peak potential. The LOD and LOQ of the recognized method positively competed well with many spectrometric [4–15, 49, 50] and electroanalytical methods [2, 22–33]. Representative data are summarized in Table 1. Some of these methods suffered from serious interference by halide ions, the need of expert for operations, use of costly carcinogenic organic solvents and high LOD. However, the proposed method permits to evaluate lower Pd contents than the allowable level of Pd in sewage (18 to 260 µg/kg), soil (<0.7 to 47 µg/kg) as set by WHO [3, 51]. The LOD of the established method competed favorably with the LOD of the standard flame atomic absorption spectrometry (**FAAS**) (1.24 µg/L) and graphite furnace atomic absorption spectrometry (**GFAAS**) (0.4 µg/L) techniques at the optimized operational parameters.

Selectivity. The validity of the established SW CSV method was tested by studying the selectivity of TAR reagent toward Pd^{2+} (5 µg/L) in the presence of many concurrent diverse ions such as Ba^{2+}, Ca^{2+}, Mg^{2+}, Cd^{2+}, Co^{2+}, Fe^{2+}, Fe^{3+}, Mn^{2+}, Ni^{2+}, Pb^{2+}, Zn^{2+}, Al^{3+}, AsO_2^-, AsO_3^- SbO_2^-, SbO_3^- or Si^{4+} individually at high concentrations (up to 500 µg/L). The acceptance limit corresponds to the concentration of the diverse ion added causing a relative error of ±4% in the peak current signal at −0.43 V versus Ag/AgCl. The results revealed no reactivity at all to most of the tested ions, whereas weak interaction was noticed toward Ca^{2+}, Ba^{2+}, Fe^{2+} and Al^{3+}. Thus, it can be assumed that the stability of complexes of these ions toward TAR is much lower than that of Pd–TAR. Interference of Ca^{2+} and Ba^{2+} was masked by adding few drops of EDTA (0.01%, w/v). The interference of Al^{3+} was masked by addition of few drops of NaF (0.001%, w/v), whereas the effect of Fe^{2+} was minimized by oxidation with few drops of H_2O_2 (20%, v/v) in the presence of NaF. The selectivity of the established method was also tested in the presence of excess (up to

10 µg/mL) of selected surfactants, e.g., sodium dodecyl sulfate, tetraheptylammonium chloride and Triton X-100, in water as "model" surfactants under the optimized parameters. The data revealed their negligible interference on palladium determination using TAR. These results revealed the high affinity and selectivity of TAR toward Pd^{2+} at the optimized parameters.

Robustness. Robustness of the established method was evaluated by measuring the cathodic peak current after minor changes in the analytical parameters, e.g., pH from 7.0 to 8.0, deposition time from 200 to 220 s, accumulation potential from 0.12 to 15 V and TAR concentration under the recommended parameters. The data revealed no significant differences (less than ±5%) in the measured current values at the optimized procedures (I_1) and after slight changes in the tested parameters confirming the analytical utility of the method. Acceptable relative standard deviation (**RSD**) in the range 3.0–3.5% and percent recovery (95–98%) were achieved as observed from the deviation in the cathodic peak current. At a 95% confidence ($n = 3$), the data were further subjected to the Student t test and the values of the experimental t_{exp} (0.16–1.9) test were lower than the critical t_{crit} (3.18) revealing the analytical utility of the established method.

Validation and analytical applications of the established methodology. *Determination of Pd in certified reference material.* Validation of the proposed SW CSV method was assessed by Pd determination in CRM (IAEA Soil-7) using the standard addition procures. Under the optimized parameters, the measured $i_{p,c}$ at $E_{p,c}$ −0.43 V increased linearly at various standard additions of Pd^{2+} (0–15 µg/L). The results achieved by the established method and ICP-MS are given in Table 2. The estimated Pd^{2+} recovery and RSDs are satisfactory. The experimental Student t_{exp} (1.84) and F_{exp} (4.24) values at a 95% confidence ($n = 5$) did not

Table 2. Analytical results for palladium(II) determination in CRM and road dust samples by the proposed SW CSV (A) and ICP−MS (B)[a]

Sample	Added, ng/g	Found, ng/g		Recovery, %
		A	B	
IAEA Soil-7 (CRM)	0	−	−	−
	5	4.88 ± 0.03	5.0 ± 0.1	97.6 ± 1.0
	10	9.50 ± 0.05	9.8 ± 0.1	95.0 ± 0.5
	15	14.20 ± 0.08	15.5 ± 0.3	94.7 ± 0.6
Roadside dust	0	−	−	−
	5	4.90 ± 0.06	5.08 ± 0.05	98.0 ± 1.2
	10	10.30 ± 0.07	10.10 ± 0.07	103.0 ± 0.7
	15	14.87 ± 0.07	15.30 ± 0.08	99.1 ± 0.5

[a]Calculated respective regression equations $\pm$ standard deviation. The experimental Student t_{exp} (1.56−1.84) and F_{exp} values (4.24−4.54) at a 95% confidence ($n = 5$) did not exceed the tabulated Student t_{tab} (2.78) and F_{tab} (6.39) values, respectively.

exceed the tabulated Student t_{tab} (2.78) and F_{tab} (6.39) values [52], respectively, confirming the precision and independency on the matrix interference.

Determination of Pd in road dust. The established SW CSV method was also successfully applied for the determination of Pd^{2+} in road dust sample as described in the experimental section. The analytical data of Pd^{2+} determination by the proposed SW CSV were close to the ICP−MS results (Table 2). Satisfactorily recovery of the spiked Pd^{2+} was achieved revealing validation of the established SW CSV procedure for Pd determination in a complex matrix. The experimental Student t_{exp} (1.56) and F_{exp} values (4.54) at $P = 0.05$ ($n = 5$) were found lower than the tabulated Student t

Table 3. Determination of palladium(II) in various water samples by the developed SW CSV and ICP−MS methods[a]

Sample	Added, μg/L	Found ± SD, μg/L	Recovery ± RSD, %
Tap water	0	nd[b]	−
	10	10.90 ± 0.13 (10.2 ± 0.3)	109.0 ± 1.2
	20	20.70 ± 0.18 (19.7 ± 0.3)	103.5 ± 0.9
	30	29.60 ± 0.17 (30.7 ± 0.5)	102.0 ± 0.6
Waste water	0	nd (0.14 ± 0.07)	−
	20	20.43 ± 0.19 (19.80 ± 0.22)	103.5 ± 0.9
	40	41.40 ± 0.21 (39.20 ± 0.23)	101.5 ± 0.5

[a]ICP−MS data are given in parentheses ($n = 3$) and [b]nd = not detected.

and F values [52], respectively, supporting the analytical performance of the developed method.

Determination of Pd in environmental water samples. To study the potential of the established SW CSV based assay for Pd determination, a recovery test was performed for Pd in environmental water samples. Collected water samples were spiked with different concentrations (0−30 μg/L) and analyzed as described earlier. The results for trace determination of Pd^{2+} in tap water are summarized in Table 3. The $i_{p,c}$ increased with increasing Pd^{2+} concentrations and the added and found values of Pd^{2+} concentrations were comparable and satisfactorily recoveries of Pd^{2+} in tap water (from 102.0 ± 0.6 to $109.0 \pm 1.2\%$) and wastewater (from 101.5 ± 0.5 to $103.0 \pm 0.9\%$) were achieved as given in Table 3. In water samples (Table 3), the data for Pd(II) determination are overestimated compared to the results achieved by the reference method. The high sensitivity of the HMDE toward matrix interference in the water samples may participate in Pd^{2+} recovery in wastewater and a slight deviation was noticed compared to tap water. Moreover, a slight shift in the $E_{p,c}$ was also noticed due to the matrix complexity and the presence of organic matter in the wastewater samples. Pd recovery in the water samples by the proposed SW CSV was close to ICP−MS results confirming the suitability and validity of the present SW CSV method for Pd determination in real samples. Thus, the developed method can be implemented for rapid quantification of Pd^{2+} in water samples with complex matrices.

CONCLUSIONS

The proposed SW CSV method at the HMDE offers a precise, reliable, convenient and robust tool for the quantification of trace Pd levels. The LOD of the developed technique is lower than the maximum allowable level for Pd set by WHO in surface

(100 μg/L) and drinking (5 μg/L) water [3, 47] and compared with LOD of many spectrochemical, e.g., GFAAS, FAAS and ICP–MS, and electrochemical techniques (Table 1). The method can be extended for ultra trace (ng/g or ng/mL) quantification of Pd^{2+} in water samples with prior preconcentration of Pd^{2+} ions from a large volume of water onto solid sorbent packed column [53] or using supramolecular solvent dispersive liquid−liquid microextraction based on solidification of floating drop [54] and subsequent SW CSV determination. The attractive properties of HMDE may enable its application in different sensing areas. The technique is unsuitable when the number of influential factors is relatively large, and a systematic approach does not show the interaction among the experimental parameters. Thus, experimental design is highly recommended in the future work, since the number of parameters is large, and a systematic approach does not show the interaction among trial parameters.

FUNDING

CONFLICT OF INTEREST

The authors declare that they have no conflict of interest.

REFERENCES

1. Rezaee, M., Shadaniyan, R., Hosseini, M.H., and Khalilian, F., *Quim. Nova*, 2015, vol. 38, no. 4, p. 1678.

2. Ba-Shami, R.M., Gazzaz, H., Bashammakh, A.S., Al-Sibaai, A.A., and El-Shahawi, M.S., *Anal. Methods*, 2014, vol. 6, p. 6997.

3. Environmental Health Criteria 226, World Health Organization (WHO), Geneva, 2002.

4. Azmi, S.N.H., Iqbal, B., Al Ruqishi, B.H.K., Al Sayabi, S.A.M., Al Quraini, N.M.K., and Rahman, N., *J. Assoc. Arab Univ. Basic Appl. Sci.*, 2016, vol. 19, p. 29.

5. Dong, X., Han, Y., Hu, Q., Chen, J., and Yang, G., *J. Braz. Chem. Soc.*, 2006, vol. 17, no.1, p. 189.

6. Asimellis, G., Michos, N., Fasaki, I., and Kompitsas, M., *Spectrochim. Acta, Part B*, 2008, vol. 63, p. 1338.

7. Dadfarnia, S., Shabani, A.M.H., and Amirkavei, M., *Turk. J. Chem.*, 2013, vol. 37, p. 746.

8. Jamali, M.R., Assadi, Y., and Kozani, R.R., *J. Chem.*, 2013, vol. 1, p. 6.

9. Shokrollahi, A. and Ramdar, K., *J. Taibah Univ. Sci.*, 2017, vol. 11, no. 5, p. 782.

10. Sacmaci, S. and Kartal, S., *Talanta*, 2013, vol. 109, p. 26.

11. Mohamadi, M. and Mostafavi, A., *Talanta*, 2010, vol. 81, p. 309.

12. Majidi, B. and Shemirani, F., *Talanta*, 2012, vol. 93, p. 245.

13. Liang, P., Zhao, E., and Li, F., *Talanta*, 2009, vol. 77, p. 1854.

14. Kokya, T.A. and Farhadi, K., *J. Hazard. Mater.*, 2009, vol. 169, nos. 1−3, p. 726.

15. Kovachev, N., Sanchez, A., Simitchiev, K., Stefanova, V., Kmetov, and Canals, V.A., *Int. J. Environ. Anal. Chem.*, 2012, vol. 92, no. 9, p. 1106.

16. Puls, C., Limbeck, A., and Hann, S., *Atmos. Environ.*, 2012, vol. 55, p. 213.

17. Jaison, P.G., Kumar, P., Telmore, V.M., and Aggarwal, S.K., *Rapid Commun. Mass Spectrom.*, 2012, vol. 26, no. 17, p. 1971.

18. Ye, Y.-Q., Yang, X.-Z., Li, X.-S., Yao, F.-Q., and Hu, Q.-F., *Asian J. Chem.*, 2012, vol. 24, no. 11, p. 4967.

19. Yin, Q.H., Zhu, D.M., Yang, D.Z., Hu, Q.F., and Yanga, Y.L., *J. Appl. Spectrosc.*, 2018, vol. 84, no. 6, p. 1084.

20. Volovenko, O., Keda, T., Skreminska, N., Milokhov, D., Khilya, O., and Zaporozhets, O., *Ads. Sci. Technol.*, 2017, vol. 35, nos. 7−8, p. 728.

21. Mahapatra, A.K., Manna, S.K., Maiti, K., Mondal, S., Maji, R., Mandal, D., Mandal, S., Uddin, M.R., Goswami, S., Quah, C.K., and Fun, H.-K., *Analyst*, 2015, vol. 140, p. 1229.

22. Locatelli, C., *Electroanalysis*, 2007, vol. 19, p. 2167.

23. Kim, S.I. and Cha, K.W., *Talanta*, 2002, vol. 57, p. 675.

24. Georgieva, M. and Pihlar, B., *Electroanalysis*, 1996, vol. 8, no. 12, p. 1155.

25. Abiman, P., Wildgoose, G.G., Xiao, L., and Compton, R.G., *Electroanalysis*, 2008, vol. 20, p. 1607.

26. Locatelli, C., Melucci, D., and Torsi, G., *Anal. Bioanal. Chem.*, 2005, vol. 382, p. 1567.

27. Locatelli, C., *Electrochim. Acta*, 2006, vol. 52, p. 614.

28. Locatelli, C., *Anal. Chim. Acta*, 2006, vol. 557, p. 70.

29. Locatelli, C., *Electroanalysis*, 2007, vol. 19, p. 445.

30. Sladkov, V.E., Prokhorova, G.V., and Ivanov, V.M., *J. Anal. Chem.*, 2000, vol. 55, no. 9, p. 889.

31. Locatelli, C., *Electroanalysis*, 2005, vol. 17, no. 2, p. 140.

32. Aher, V.T., Palrecha, M.M., Kulkarni, A.V., and Shah, G.C., *J. Radioanal. Nucl. Chem.*, 2002, vol. 252, no. 3, p. 573.

33. Velmurugan, M., Thirumalraj, B., Chen, S-M., Al-Hemaid, F.M.A., Ali, M.A., and Elshikh, M.S., *J. Colloid Interface Sci.*, 2017, vol. 485, p. 123.

34. Yilmaz, U.T. and Inan, D., *J. Food Sci. Technol.*, 2015, vol. 52, no. 10, p. 6671.

35. Melo, L.C., Julião, M.S., and Milhome, M.A., do Nascimento, R.F., De Souza, D., de Lima-Neto, P., and Correia, A.N., *J. Anal. Chem.*, 2018, vol. 73, no. 7, p. 695.

36. Fischer, E. and Van Den Berg, C.M.C., *Anal. Chim. Acta*, 2001, vol. 432, no. 1, p. 11.

37. Yokio, K., Yamaguchi, A., Mizumachi, M., and Koide, T., *Anal. Chim. Acta*, 1995, vol. 316, no. 3, p. 363.

38. Narin, I. and Soylak, M., *Fresenius Environ. Bull.*, 1999, vol. 8, nos. 1–2, p. 14.

39. Sawyer, D., Heinemann, W.R., and Beebe, J., *Chemistry Experiments for Instrumental Methods*, New York: Wiley, 1984.

40. Nakamoto, K., *Infrared and Raman Spectra of Inorganic and Coordination Compound*, New York: Wiley, 1971.

41. Rusu, A., Hancu, G., Toth, G., Toma, E., Toma, F., Mare, A., Man, A., Velescu, B.S., and Uivarosi, V., *Farmacia*, 2016, vol. 64, no. 6, p. 922.

42. Menek, N., Basaran, S., Turgut, G., and Odabasoglu, M., *Dyes Pigm.*, 2004, vol. 61, p. 85.

43. Nicholson, R.S. and Shain, I., *Anal. Chem.*, 1964, vol. 36, no. 4, p. 706.

44. Parajoin-Costa, B.S., Gonzalez-Baro, A.C., and Baran, E.J., *Z. Anorg. Allg. Chem.*, 2002, vol. 628, p. 1419.

45. Bard, A.J. and Faulkner, L.R., *Electrochemical Methods: Fundamentals and Applications*, New York: Wiley, 2001, 2nd ed.

46. Guidelli, R., Compton, R.G., Feliu, J.M., Gileadi, E., Lipowski, J., Schmickler, W., and Trasatti, S., *Pure Appl. Chem.*, 2014, vol. 86, no. 2, p. 245.

47. Laviron, E., *J. Electroanal. Chem.*, 1979, vol. 101, p. 19.

48. Konieczka, P. and Namieśnik, J., *Quality Assurance and Qquality Control in the Analytical Chemical Laboratory: A Practical Approach*, Boca Raton: CRC, 2009.

49. Li, C., Chai, C., Xiaolin, L., and Mao, X., *Geostand. Geoanal. Res.*, 2007, vol. 22, no. 2, p. 195.

50. Bagheri, A., Behbahani, M., Amini, M.M., Sadeghi, O., Tootoonchi, A., and Dahaghin, Z., *Microchim. Acta*, 2012, vol. 178, p. 261.

51. Nordberg, G.F., Fowler, B.A., Nordberg, M., and Friberg, L.T., *Handbook on the Toxicology of Metals*, New York: Academic, 2007, 3rd ed.

52. Miller, J.N. and Miller, J.C., *Statistics and Chemometrics for Analytical Chemistry*, London: Pearson Education, 2010, 6th ed.

53. Farag, A.B., Soliman, M.H., Abdel-Rasoul, O.S., and El-Shahawi, M.S., *Anal. Chim. Acta*, 2007, vol. 601, p. 218.

54. Liang, P., Yang, E., Yu, J., and Wen, L., *Anal. Methods*, 2014, vol. 6, p. 3729.